Biochimica et Biophysica Acta xxx (2013) xxx–xxx

Contents lists available at ScienceDirect

Biochimica et Biophysica Acta

journal homepage: www.elsevier.com/locate/bbamem

Atypical surface behavior of ceramides with nonhydroxy and 2-hydroxy very long-chain (C28–C32) PUFAs

Daniel A. Peñalva [a], Gerardo M. Oresti [a], Fernando Dupuy [b], Silvia S. Antollini [a], Bruno Maggio [b], Marta I. Aveldaño [a], María L. Fanani [b,*]

[a] Instituto de Investigaciones Bioquímicas de Bahía Blanca (INIBIBB), Universidad Nacional del Sur and Consejo Nacional de Investigaciones Científicas y Técnicas (CONICET), 8000 Bahía Blanca, Argentina

[b] Departamento de Química Biológica, Centro de Investigaciones en Química Biológica de Córdoba (CIQUIBIC), Facultad de Ciencias Químicas, Universidad Nacional de Córdoba and CONICET, 5000 Córdoba, Argentina

ARTICLE INFO

Article history:
Received 15 August 2013
Received in revised form 7 November 2013
Accepted 26 November 2013
Available online xxxx

Keywords:
2-Hydroxy fatty acids
Brewster angle microscopy
Langmuir monolayers
Two dimensional phase transitions
Sphingolipids

ABSTRACT

Unique species of ceramide (Cer) with very-long-chain polyunsaturated fatty acid (VLCPUFA), mainly 28–32 carbon atoms, 4–5 double bonds, in nonhydroxy and 2-hydroxy forms (n-V Cer and h-V Cer, respectively), are generated in rat spermatozoa from the corresponding sphingomyelins during the acrosomal reaction. The aim of this study was to determine the properties of these sperm-distinctive ceramides in Langmuir monolayers. Individual Cer species were isolated by HPLC and subjected to analysis of surface pressure, surface potential, and Brewster angle microscopy (BAM) as a function of molecular packing. In comparison with known species of Cer, n-V Cer and h-V Cer species showed much larger mean molecular areas and increased molecular dipole moments in liquid expanded phases, which suggest bending and partial hydration of the double bonded portion of the VLCPUFA. The presence of the 2-hydoxyl group induced a closer molecular packing in h-V Cer than in their chain-matched n-V Cer. In addition, all these Cer species showed liquid-expanded to liquid-condensed transitions at room temperature. Existence of domain segregation was confirmed by BAM. Additionally, thermodynamic analysis suggests a phase transition close to the physiological temperature for VLCPUFA-Cers if organized as bulk dispersions.

1. Introduction

Intensive research over the past decades has implicated ceramide (Cer) in the regulation of a great variety of key cellular functions. However, the paradigm that a single Cer species is responsible for many different cell functions has been challenged by the recognition that "ceramide" constitutes a family of related molecules, subject to metabolism by nearly 30 enzymes and with dozens of structurally distinct molecular species [15]. Saturated and monounsaturated fatty acids from C_{14} to C_{24} are typical acyl chains of sphingolipids in most mammalian tissues, although shorter chain ceramides originated from various transacylation reactions also occur naturally [6]. Notable exceptions are skin and testis sphingolipids, which contains glucosyl-Cer species with fatty acids up to C_{34} long [39] and mammalian testis and spermatozoa, which have sphingomyelin (SM) and Cer with high proportions of very long chain (C_{24} to C_{36}) polyunsaturated fatty acids (VLCPUFA) of the n−6 or the n−3 series [12,35], i.e., elongated versions of well-known C20 or C22 PUFA of the n−6 or the n−3 series, such as arachidonic, docosapentaenoic or docosahexaenoic acids.

In many tissues, of which myelin and skin sphingolipids are known examples, an important part of the sphingolipid species contains a 2-hydroxyl group at the second carbon atom of their fatty acyl chain [14]. This biochemical modification also occurs in the VLCPUFA of rodent testis sphingolipids including SM [37], gangliosides [36,40], and Cer [43]. In rat testis, the ratio between 2-hydroxy and nonhydroxy VLCPUFA (h-V and n-V, respectively) in SM and Cer increases from the onset of spermatogenesis to adulthood [43]. This is due to the fact that n-V Cer and SM species are exclusive components of precursor spermatocytes, whereas h-V Cer and SM species appear as they differentiate to spermatids, as well as in spermatozoa [43]. In mature gametes, n-V SM and h-V SM, but no Cer, occur endogenously on the sperm head and, intriguingly, considerable amounts of solely h-V Cer species are located on the tail [30]. Almost complete hydrolysis of the head-located SM occurs after inducing the acrosomal reaction [44], this leading to gametes that are considerably enriched in n-V, and especially in h-V, ceramides. Thus, whereas in testicular germ cells VLCPUFA-containing ceramides play a role as biosynthetic precursors

Abbreviations: Cer, ceramide; VLCPUFA, very long chain polyunsaturated fatty acid; h-V, 2-hydroxy VLCPUFA; n-V, nonhydroxy VLCPUFA; SM, sphingomyelin; $\mu_\perp$, dipole moment perpendicular to the interface; π, surface pressure; π_t, transition pressure; ΔV, surface potential; BAM, Brewster angle microscopy; Cs^{-1}, compressibility modulus; LC, liquid-condensed; LE, liquid-expanded; MMA, mean molecular area; S, solid phase; *L*, semi-empirical average molecular length; *V*, semi-empirical molecular volume; *Th*, semi-empirical film thickness

* Corresponding author at: CIQUIBIC, UNC-CONICET, Haya de la Torre y Medina Allende, Ciudad Universitaria, X5000HUA Córdoba, Argentina. Tel.: +54 351 4334168; fax: +54 351 4334074.
E-mail address: lfanani@fcq.unc.edu.ar (M.L. Fanani).

0005-2736/$ – see front matter © 2013 Published by Elsevier B.V.
http://dx.doi.org/10.1016/j.bbamem.2013.11.018

of complex sphingolipids including SM, in acrosome-reacted spermatozoa they are final products. Based on previous studies on different species of SM being converted to Cer by the action of sphingomyelinase [8,19,38], such a massive increase in the Cer/SM mole ratio may be envisaged to have an important impact on the sperm surface properties.

Although there are studies extensively describing Cer properties in Langmuir monolayer [4,6,7,9,18,23], the effects on lipid bilayers of diverse Cer species in pure and mixed form [34], and the impact of actively generating Cer from SM by sphingomyelinase on different features of the membrane physical state [8,19,38], the properties and behavior of the relatively novel n-V and h-V Cer species remain to be established. The aim of this study was to define specific molecular parameters of individual molecular species of these sperm-associated Cers, as well as their thermodynamic properties. In Langmuir monolayers, surface pressure, surface potential, and imaging by Brewster angle microscopy (BAM) were measured to determine their average molecular organization at the membrane interface. Our results showed that n-V Cer species differ significantly from h-V Cer species in most of their surface properties and that both behave atypically if compared with the more ubiquitous molecular species of Cer previously described in the literature [6].

2. Materials and methods

2.1. Chemicals

16:0 Cer, 18:1 Cer, 24:1 Cer and 2-hydroxy 24:0 Cer were from Avanti Polar Lipids Co (Alabaster, AL). The n-V Cer and h-V Cer were obtained from adult Wistar rat testes using a combination of TLC and HPLC procedures. The silica gel was from Merck, the HPLC column was from Rainin LC. The gas chromatography and HPLC equipments were both from Varian Inc., USA. All solvents were HPLC grade (JT Baker; UVE, Dorwill, Argentina).

2.2. Separation of ceramides

Lipid extracts were prepared from rat testes [2] and spotted on 500 μm-silica gel TLC plates under N_2 along with commercial standards. Chloroform:methanol:ammonia (90:10:2, by vol.) resolved rat testis Cer into two bands. The lower one was almost exclusively made up by h-V Cer species, whereas the upper one contained all Cer species with nonhydroxy fatty acids, this including common Cer species with C_{16} to C_{26} fatty acids and those with nonhydroxy VLCPUFA [43]. The separated h-V and n-V fractions were recovered and treated with N_2-saturated 0.5 N NaOH in anhydrous methanol at 50 °C for 10 min in order to remove any potential lipid contaminant with ester-bounded fatty acids from the Cer samples, neutralized, partitioned into chloroform, and subjected again to TLC. This time chloroform:methanol:ammonia:water (90:10:05:0.5, by vol.) was used, as it allows the fraction containing Cer species with C_{16} to C_{26} fatty acids to lag behind the Cer species containing nonhydroxy VLCPUFA [11]; this propensity facilitates partial purification of the latter.

Silica gel plates impregnated with 10% $AgNO_3$ and chloroform:methanol (80:20, by vol.) were then used to separate the Cer species with C_{16} to C_{26} fatty acids from those containing VLCPUFA. This resulted in partial resolution of the latter ceramides into two bands: the upper one contained the main very long chain tetraenoic fatty acid (n−28:4) and the lower one mainly the pentaenoic fatty acids (n−30:5 and n−32:5). Although with the expectedly lower Rf values due to the hydroxyl group, an essentially similar separation resulted when h-V Cers were subjected to this procedure. After this pre-separation, each of the Cer subfractions was subjected to HPLC to obtain the six major VLCPUFA-containing Cer species from rat testis (Fig. 1).

Lipids were located on TLC plates under UV light after spraying with 2,7-dichlorofluorescein, and rapidly transferred to glass tubes for elution. This was done by successively extracting the silica with nitrogen-saturated chloroform:methanol:water (5:5:1), centrifuging, collecting the supernatants, and partitioning them with 4.5 volumes of water [2]. The eluates were finally washed with methanol:1 M NaCl (1:1 by vol.) to remove Ag^+ ions. The organic phases were reduced in volume under N_2, filtered to remove traces of particulate matter, dried, and dissolved in methanol for HPLC injection.

HPLC was performed at 35 °C using a stainless steel column (250 mm × 4.6 mm ID) packed with 5 μm particles covered with octylsilane (C8). The solvent, at a flow rate of 1 mL/min was methanol:1 mM potassium phosphate buffer, pH 7.4, in a 96:4 (v/v) ratio. Cer peaks were detected at 205 nm using a Prostar 335 photodiode array detector and collected as they emerged from the column. Chloroform and water were then added to the eluates and Cer species were recovered in the chloroform phase resulting after phase partition.

Individual species were identified and quantified by means of gas chromatography after adding appropriate amounts of n−16:0 Cer and h−24:0 (2S–OH) as internal standards to the samples, subjecting them to methanolysis, and recovering by TLC the nonhydroxy and 2-hydroxy fatty acid methyl esters to be subjected to GC. The former were analyzed directly and the latter after conversion into trimethyl–silyl derivatives [29,43].

2.3. Monolayer compression isotherms

Langmuir isotherms were obtained using a 90 cm^2 compartment of a specially designed circular Monofilmmeter Teflon trough (Mayer Feintechnik, Germany) filled with 80 mL of 145 mM NaCl, pH ~5.6, equipped with a platinized Pt plate for measuring the surface pressure. The surface potential of the film was simultaneously measured by a surface ionizing electrode formed by a ^{241}Am plate positioned 5 mm above the monolayer surface, and a reference calomel electrode connected to the aqueous subphase.

The whole system was enclosed in an acrylic box, saturated with N_2 gas to prevent lipid peroxidation, and surrounded by a metallic grid connected to ground to reduce external interference in surface potential measurements. Experiments were performed using a subphase of 145 mM NaCl kept at 21 °C and 8 °C (±0.5 °C) by means of an external circulating water bath (Haake F3C). Absence of surface active impurities in the subphase solution or the spreading solvent was ascertained as described elsewhere [32].

Lipid monolayers were obtained by spreading adequate aliquots of Cer solutions onto the aqueous surface. After allowing solvent evaporation for 5 min, the surface pressure–area isotherms were

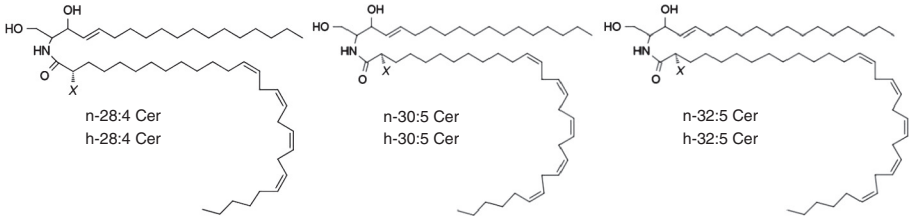

Fig. 1. Schematic structures of the ceramides (Cer) containing nonhydroxy (n) and 2-hydroxy (h) very-long-chain polyunsaturated fatty acids (VLCPUFA) studied in this work. *X* represents the presence of −H or −OH, respectively, in the second carbon atom of the amide-bound fatty acid. The depictions are shown for illustrative purposes and are not meant to represent the molecular organization adopted by the chains at the interface.

Please cite this article as: D.A. Peñalva, et al., Atypical surface behavior of ceramides with nonhydroxy and 2-hydroxy very long-chain (C28–C32) PUFAs, Biochim. Biophys. Acta (2013), http://dx.doi.org/10.1016/j.bbamem.2013.11.018

recorded while compressing the monolayers at a constant speed of 2 $Å^2$ $molecule^{-1}$ min^{-1}. The collapse pressures and limiting mean molecular areas of the Cer films were estimated by the third derivative methods [3]. Compressibility modulus (Cs^{-1}) [13] was as:

$$Cs^{-1} = -MMA(\partial\pi/\partial MMA)_T, \quad (1)$$

where MMA is the mean molecular area at a given surface pressure π.

The resultant dipole moment perpendicular to the interface ($\mu_\perp$) [13] of Cer at each molecular area was calculated from the isotherm data as:

$$\mu_\perp = \frac{1}{12\pi} MMA\Delta V, \quad (2)$$

where ΔV is the surface potential of the monolayer at the corresponding MMA, and π in this case is the mathematical Euclidean constant taken as 3.14159.

2.4. Brewster angle microscopy

BAM visualization was performed with an auto-nulling imaging ellipsometer (Nanofilm EP3sw imaging ellipsometer, Accurion GmbH, Germany) working in the BAM mode. Zero reflection was set with a polarized 532 nm laser incident on the bare aqueous surface at the experimentally calibrated Brewster angle (53.1°). After monolayer formation and compression, the reflected light was collected with a 20× objective and a CCD camera, which operates at a resolution of 1 μm. The gray level of each section of the micrograph is proportional to the reflected light intensity, which is a function of both the film thickness and its refraction index [21].

3. Results and discussion

3.1. Isolation of VLCPUFA-containing ceramide species

The procedure we used to isolate the six major VLCPUFA-containing Cer species (Fig. 1) whose properties are explored in this study was based on a recently described method applied to isolate nonhydroxy and 2-hydroxy VLCPUFA-containing species of SM from rat testis [31]. Whereas the high polarity of the phosphoryl–choline headgroup in SM imposed a difficulty for the separation of the species containing a hydroxyl group from their non-hydroxylated analogs by silica-based TLC, the h-V Cer and h-V Cer species were easily separated using silica gel as support. As previously shown [43], the h-V Cer species lag well behind the subfraction containing nonhydroxy fatty acids, and are detected as a single sharp band because it is composed almost exclusively by Cer species containing 2-hydroxy VLCPUFA. In contrast, the Cer species with nonhydroxy fatty acids tend to separate into bands according to the length of their fatty chains. Of these bands, the one grouping the Cer species with nonhydroxy VLCPUFA tends to migrate ahead from species containing shorter, mostly saturated and some monoenoic (C_{16}–C_{26}) fatty acids [12]. In preliminary HPLC separations, we found that Cer species with 24:0 or 24:1 tended to co-elute with some of the species containing C_{28}–C_{30} VLCPUFA of our interest; for this reason we decided to directly eliminate them from our samples using argentation TLC (Ag-TLC).

The high degree of unsaturation of the VLCPUFA-rich Cer species with respect to the common (C_{16}–C_{26}) ceramides was advantageous, not only to separate the former from the latter using Ag-TLC, but to detect the former with a good sensitivity when subjected to HPLC (Fig. 2). In contrast to the case of SM, for which species with very-long-chain tetraenoic and pentaenoic fatty acids are hard to separate by Ag-TLC, Cer species containing these fatty acids tended to separate according to the degree of unsaturation of the fatty acid when subjected to this procedure. Although this pre-separation implied a more laborious procedure, since more samples had to be eluted and injected, it facilitated the isolation of Cer species according to their fatty acid chain length and number of double bonds, as shown in Fig. 2.

The reverse-phase HPLC procedure previously devised to separate SMs also separated Cer species in the same order, mostly determined by their fatty acids. In both cases, elution of each of the h-V species preceded that of its corresponding chain-matched n-V counterpart (e. g., h−30:5 Cer eluted before n-30:5 Cer), as expected because of the higher polarity conferred to the former by the hydroxyl group. Also,

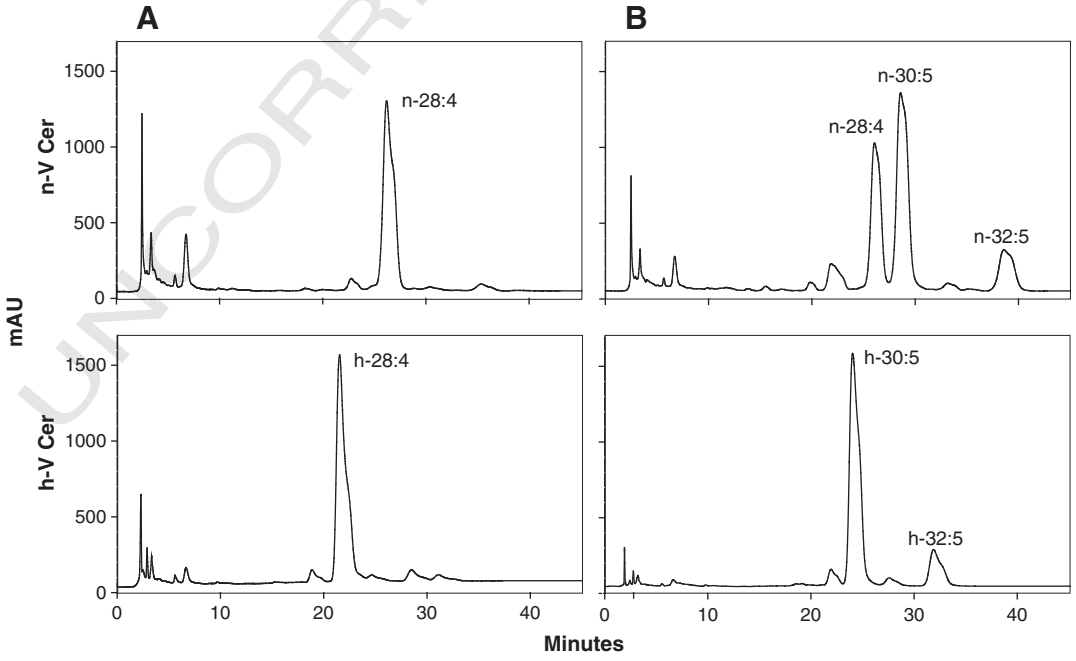

Fig. 2. Preparative isolation of VLCPUFA-containing ceramides. The nonhydroxy and 2-hydroxy VLCPUFA-containing Cer (n-V Cer and h-V Cer, respectively) were separated from rat testis by TLC and subjected to argentation TLC to isolate them from Cer species with saturated and monoenoic fatty acids. This partially resolved each the VLCPUFA-containing Cer into tetraenoic (A) and pentaenoic (B) fatty acid-containing fractions. Each of these was then separately subjected to HPLC to collect the six major (C28–C32) molecular species shown in Fig. 1. Chromatography was performed on an octylsilane column using a mobile phase of methanol–phosphate buffer flowing at 1 mL/min and a detector set at λ = 203 nm.

within h-V or n-V subfractions, species with 28:4n − 6 preceded those with 30:5n − 6 in elution order, just as free 20:4n − 6 precedes free 22:5n − 6 when they are subjected together to HPLC on reverse phase columns [1]. Thus, an additional segment of two carbon atoms in the fatty acid is more powerful in increasing the reverse phase retention of Cer than the presence of an additional double bond is in decreasing it. Most interestingly, retention times of each of the Cer species studied here (Fig. 2) were somewhat shorter than those of the corresponding SM species having chain-matched fatty acids [31], despite the high polarity the phosphorylcholine headgroup confers to the latter. Because the hydrophobicity associated to the fatty acids amide-bound to sphingosine is the same in these SM and Cer species, this relatively stronger retention may be ascribed to additional forces between the polar head group of SM and the material of the column. These could involve polar interaction of the SM charged phosphate group with free silanols or hydrophobic interactions between SM methyl groups with the covalently bound hydrophobic material. This could explain the higher symmetry of the peaks of the present Cer (Fig. 2) than of the previous SM [31] species having the same fatty acids.

3.2. Langmuir monolayers of VLCPUFA-containing Cer species

In this section, Langmuir compression isotherms of the six Cer species of this study were performed at room temperature. As shown in Fig. 3, all of them underwent a phase transition in the 5–20 mN/m pressure range, as evidenced by a kink in the plots relating mean molecular area (MMA) and surface pressure (π). At π values below 10 mN/m (or even lower in the case of h − 32:5Cer), and relatively large values of MMA, the films showed a liquid-expanded (LE) character, as emphasized by the relatively low value of the corresponding compressibility modulus (Cs^{-1}) (Table 1).

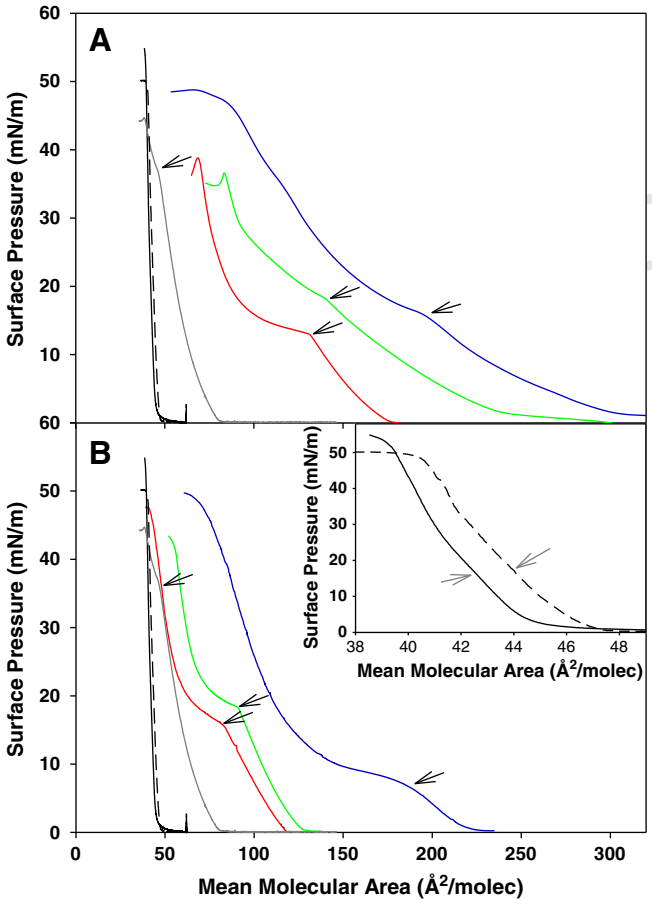

Fig. 3. Compression isotherms of n-V Cer (A) and h-V Cer (B) species. In each of the panels, the mean molecular area vs. surface pressure curves were plotted using the same symbol for each nV-Cer and the corresponding h-V Cer, as follows: n − 28:4 Cer and h − 28:4 Cer (red lines), n − 30:5 Cer and h − 30:5 Cer (green lines) and n − 32:5 Cer and h − 32:5 Cer (blue lines). For comparison, the isotherms of 24:1 Cer (black dashed line), 16:0 Cer (full black line) and 18:1 Cer (gray line) are also shown. The inset shows 16:0 Cer and 18:1 Cer in an expanded x-axis scale. The black arrows indicate the beginning of a LE → LC phase transition and the gray arrows a LC → S transition.

Cs^{-1} partially reflects the surface elasticity of the films, giving values lower than 130 mN/m for typical LE phases [22,41,42]. When the transition pressure (π_t) is reached and a LE → LC coexistence region is attained, Cs^{-1} typically drops to lower values (20–30 mN/m) and rises again when a homogeneous liquid-condensed (LC) phase is established (Table 1, see 30 mN/m). For the present VLCPUFA-containing ceramides, the π_t followed the trend: 30:5Cer > 28:4Cer > 32:5Cerin both n-V and h-V cases (Fig. 3). It is worth noting that the Cs^{-1} values for the LC phases formed by all Cer species containing VLCPUFA were lower than those obtained for other Cers, as shown for 16:0Cer and 24:1Cer in Table 1 and in [6,9,18], and also lower than that for phospholipid-LC phases, for which Cs^{-1} > 200 mN/m [22,41,42]. In comparison, at 21 °C saturated 16:0Cer organizes in a LC phase [18], which undergoes a LC → solid (S) phase transition at ~16–18 mN/m and a MMA of ~43 Å²/molecule, as shown as an inset in Fig. 3, being able to form LE phases only at higher temperatures (~35to ~48 °C) [9].

Shortening of the acyl chain, as in 12:0Cer or 10:0Cer [6], or introduction of a double bond at C9 in the amide-bound fatty acid of ceramide, as in 9Δ18:1Cer,leads to expanded monolayers which transform to condensed phases at higher π_t values than those of any of the VLCPUFA-containing ceramides examined here (see Fig. 3 and [23]). However, when the double bond occurs at the C15 of the N-linked acyl hydrocarbon chain, as in 15Δ24:1Cer, the molecules can still pack into an LC phase at room temperature [18,23] and exhibit a LC → S transition quite similar to that shown by the saturated 16:0Cer (Fig. 3 and Table 1). Counting from the amide-bound carbon, the first of the series of 4 or 5 methylene-interrupted *cis* double bonds of the Cer species of this study are located at C12, C13 and C14 in the 30:5, 28:4 and 32:5 acyl chains, respectively (Fig. 1), i.e., at an intermediate location between the two above-mentioned monounsaturated Cers. Our results indicate that VLCPUFA-containing Cer species also behave in an intermediate manner between these two species in monolayer, showing both an LE and an LC phase at room temperature (Fig. 3). The LC phase may be ascribed to their saturated portion facilitating Van der Waals interactions among acyl chains, and the LE phase to their several double bonds, promoting a more expanded behavior of these species by inducing hydrocarbon chain disordering and reducing the tightness of their packing.

A remarkable characteristic of VLCPUFA-containing Cer species was their large MMA (Fig. 3 and Table 1). Ordinary ceramides in their LC or S state typically occupy an area of ~40–42 Å²/molecule at high π (Fig. 3, inset and [4]) which is roughly the lower limiting cross-sectional area for lipids with two-tailed fully extended saturated acyl chains. However, only h − 28:4Cer and h − 30:5Cer showed MMA that were close to such value at 30 mN/m. The other Cer species with VLCPUFAshowed larger MMA values that increased with the chain length. At 10 mN/m, VLCPUFA-containing Cer followed the same tendency, occupying an area 1.5- to 3.4-fold larger than that occupied by 18:1Cer in its LE state. A comparison between each of the n-V Cer and the h-V Cer species showed that the latter packed into smaller areas (Table 1) and had more defined LE → LC transitions (Fig. 3) than the former. This reflects a better capacity for close molecular packing in h-V than in n-V Cer species, which may be ascribed to the presence of the 2-hydroxyl group near the air–water interphase.

The surface (dipole) potential (ΔV) in lipid monolayers is the resultant of several components. It includes contributions of the chemical groups of the lipid molecule to the overall resultant dipole moment perpendicular to the interface, as well as the contribution from the hydration shield associated to the polar headgroups [4,13]. As expected, ΔV measurements of the VLCPUFA-containing Cer films increased with the acyl chain length and with π. This may be ascribed to the attainment

Table 1
Characteristic parameters of VLCPUFA-containing ceramide monolayers.

Molecular species	10 mN/m				30 mN/m			
	MMA	Cs^{-1} [a]	Phase state	ΔV	MMA	Cs^{-1} [a]	Phase state	ΔV
n−28:4Cer	141 ± 4	62 ± 4	LE	248 ± 5	78 ± 4	80 ± 4	LC	379 ± 9
n−30:5Cer	182 ± 3	37 ± 2	LE	258 ± 7	102 ± 6	46 ± 14	LE–LC	301 ± 10
n−32:5Cer	222 ± 3	37 ± 2	LE	306 ± 7	125 ± 2	50 ± 2	LC	380 ± 7
h−28:4Cer	101 ± 3	56 ± 6	LE	172 ± 1	58 ± 4	74 ± 9	LC	248 ± 1
h−30:5Cer	106 ± 2	69 ± 9	LE	168 ± 4	60 ± 1	93 ± 7	LC	257 ± 4
h−32:5Cer	140 ± 5	20 ± 6	LE–LC	215 ± 5	97 ± 3	71 ± 8	LC	266 ± 4
n−16:0Cer	43 ± 2	307 ± 10	LC	475 ± 6	41 ± 1	433 ± 10	S	513 ± 20
n−18:1Cer	65 ± 3	59 ± 7	LE	237 ± 5	50 ± 2	91 ± 6	LE	274 ± 6
n−24:1Cer	45 ± 2	644 ± 12	LC	428 ± 10	42 ± 1	904 ± 15	S	431 ± 10

[a] Calculated after Eq. (1).

of an orientation more perpendicular to the interface of the Cer molecules as the molecular density increases. However, hydration–dehydration processes under increased packing cannot be excluded, since these are also contained in this parameter. The ΔV values for the n-V Cer species in the LE state were situated in the same range as the ΔV of 18:1Cer (which is also able to form an LE phase at room temperature), whereas in the LC state they were lower than those of the condensed 16:0 Cer and 24:1 Cer (Table 1 and [18]). It is remarkable that the n-V Cer species showed higher ΔV values than the h-V Cer species even when such values corresponded to lower molecular densities, considering that the MMA of the n-V Cer species were in all cases larger than those of the corresponding h-V Cer species. This phenomenon may reflect chain conformational differences between those two groups and is discussed further below.

3.3. BAM visualization of monolayers of VLCPUFA-containing ceramides

The surface topography of monolayers of VLCPUFA Cer at the air–water interface was inspected by Brewster angle microscopy (BAM). This technique allows visualization and partial identification of the different lipid phases because of contrasts derived from intrinsic physical properties such as refraction index and interfacial thickness. In general, LC phases appear brighter than LE phases (increased surface reflectivity) as they show a higher refraction index and/or film thickness [6]. Fig. 4 shows BAM images of the VLCPUFA-containing Cer films at the π region where there is LE–LC coexistence. The appearance of LC domains was observed in all but in the n-30:5 Cer film, which showed a very diffuse phase transition at 23 ± 2 mN/m. This may correspond either to two optically similar phases, not different enough in reflectivity to be visualized, or to the formation of LC domains that were too small to be resolved by the microscope.

The rest of the VLCPUFA-containingCer monolayers revealed the occurrence of small LC domains a few mN/m above their π_t which grew upon film compression forming flower-like bright domains that remained separated until most of the film area became LC (Fig. 4). This behavior was observed previously for other Cer species [6] and is characteristic of the formation of an LC phase with a higher surface potential than that of the LE phase (see Table 1). This induces an intra-domain molecular dipole repulsion that leads to adoption of non-circular domain shapes [28], with higher order dipolar repulsion being sensed at long ranges as inducing an inter-domain repulsion that prevents Cer domains to coalesce and leads them to dispose in a rather organized lattice [16].

3.4. Estimation of ceramide organization in monolayers

At this point the question arose whether these lipids, having such large acyl chains, are organized as rather thick films. BAM reflectivity is proportional to the film thickness, but since it also depends on the film refraction index and their separate contributions cannot be assessed with certainty, this question was approached from an indirect point of view. The average volume and length of an acyl chain has been empirically evaluated in early studies for both glycophospholipids and sphingolipids [20,24] and found to be expressed by the following semi-empirical laws:

$$v = 27.4 + 26.9n; \quad (3)$$

$$l = 0.8(1.5 + 1.265n) - 0.9n_{db}, \quad (4)$$

where v is the average volume of a single hydrocarbon chain, n is the number of carbon atoms in such chain, l is the length of a single chain in its maximal extension, and n_{db} is the number of double bonds in the chain.

For the present Cer species with VLCPUFA, we calculated their total average volume (V) as the sum of the volumes of their two asymmetrical chains (v) after Eq. (3), and their average chain lengths (L) as the average between the lengths of their two hydrocarbon chains (l) after Eq. (4) (Table 2). Also, taking into account the MMA measured experimentally, a semi-empirical thickness (Th) for each Cer species was calculated, as V/MMA. The Th values were smaller for all VLCPUFA-containing Cer than for 16:0 or 24:1 Cer, and smaller for n-V Cer than for their corresponding chain-matched h-V Cer (Table 2). A comparison of Th with L values should highlight some structural properties of Cer molecular organization in films. Cer Th values should closely match Cer L if molecules self-organized at their LC state with a fully extended conformation, as is the case of common saturated Cer species, whereas a low Th value with respect to L would indicate curved dispositions of their acyl chains. The lowest values of L/Th ratio were displayed by 16:0 and 24:1 Cer, followed by h−28:4 Cer and h−30:5 Cer in their LC state (Table 2). For all the other VLCPUFA Cer species in the LC phase Th values were considerably smaller than L, even by a factor of two (Table 2). This indicates that these species self-organize with a bent structure of their acyl chains in monolayer films.

Whereas the polar headgroup of Cer is small enough to fit under a transverse area section of scarcely 40 $Å^2$/molecule [6,9], the MMA values for these Cers ranged between 58 and 120 $Å^2$/molecule in the LC phase and 100–222 $Å^2$/molecule in the LE state (Table 1). Thus, an important portion of the hydrocarbon chains may be exposed to the water interface for some Cer species and phase conditions. Due to the conjugated π-orbitals, the unsaturated second portion of the VLCPUFA acyl chains bears a more polarizable nature and higher conformational degrees of freedom at the studied temperatures than the first saturated portion, and it could become partially in contact with the aqueous interface. Table 2 shows the resultant dipole moment perpendicular to the interface ($\mu_\perp$) calculated from ΔV and MMA data according to Eq. (2), which reflects the overall molecular dipole contribution to the total ΔV measurement. Two of the Cer that appeared to be in a straight conformation of their hydrocarbon chains in the LC phase as suggested by

Please cite this article as: D.A. Peñalva, et al., Atypical surface behavior of ceramides with nonhydroxy and 2-hydroxy very long-chain (C28–C32) PUFAs, Biochim. Biophys. Acta (2013), http://dx.doi.org/10.1016/j.bbamem.2013.11.018

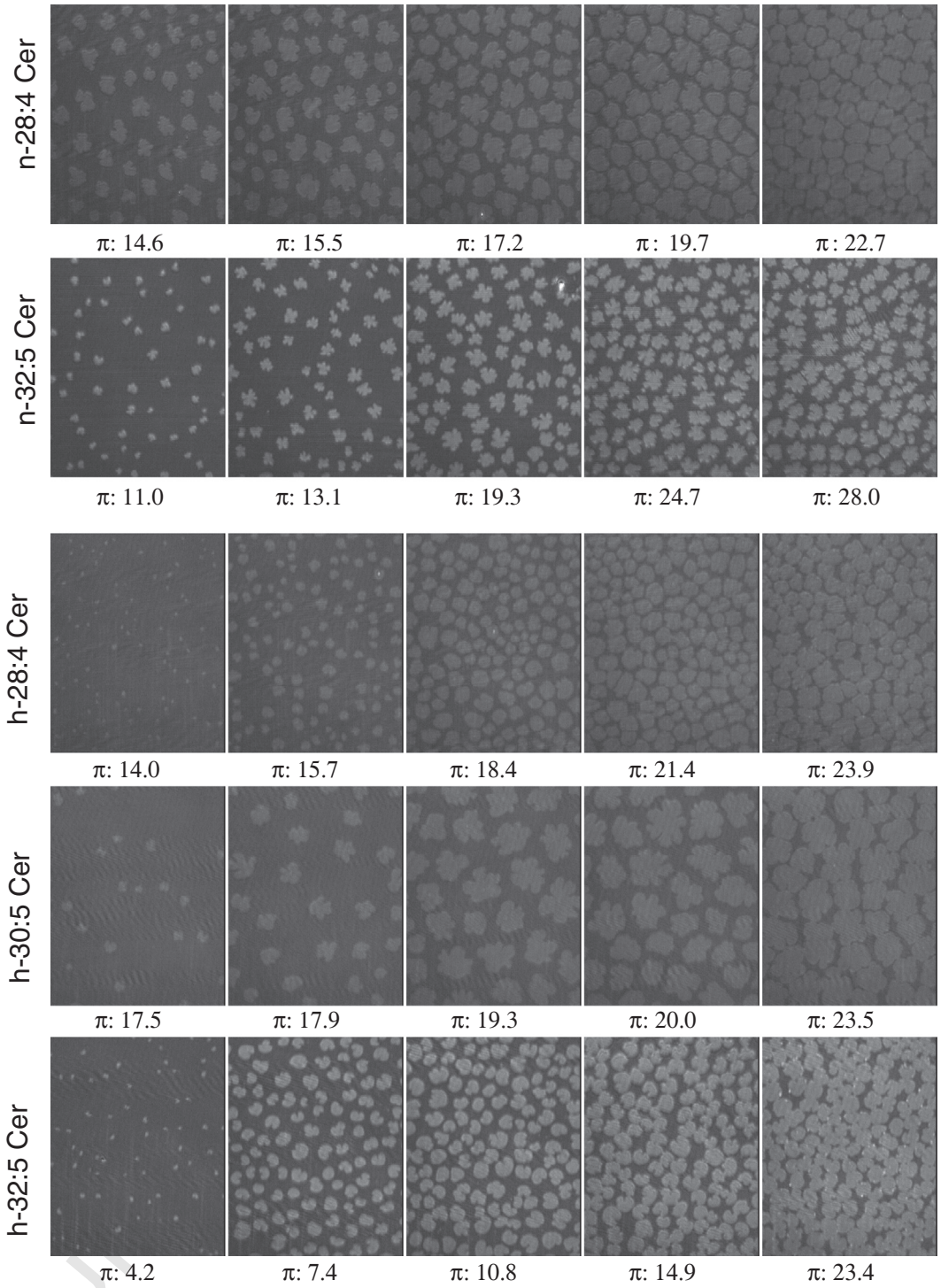

Fig. 4. Brewster angle microscopy visualization of monolayers of VLCPUFA-containing ceramides through the LE–LC transition region. The images correspond to each of the Cer species of this study at the indicated surface pressure π values. For a better visualization, the lower 0–100 gray level range (from the 0–255 original scale) was selected. The pictures are representative of two independent experiments. Image size 200 × 250 μm.

the *L/Th* analysis, h−28:4 and h−30:5 Cer, showed the lowest $\mu_{\perp}$ values of the table (~360–400 mD). These values were even lower than those exhibited for 16:0Cer and 24:1Cer in the LC state ([6,18] and Table 2) indicating a strong contribution of the chain-OH group in opposition to that of the hydrocarbon moiety. Remarkably, the n-V Cer species showed very high $\mu_{\perp}$ values, almost duplicating those of the h-V Cer species and correlating with $L/Th \gg 1$ (Table 2). It has been previously demonstrated that the introduction of a double bound in the middle portion of the acyl chain of Cer, where an isotropic electronic environment is sensed, do not affect substantially the dipole properties. However, when the double bond is sited in a region that present an asymmetric electronic environment, such as in the vicinity of the interface, the double bound contributes to enhance the dipole potential of the molecule, due both by polarization of the conjugated π-orbitals of the double bond and, likely, by interaction with water molecules [4]. Thus, the high resultant dipole moment measured for the longest VLCPUFA-Cers supports that these Cer molecules adopt a bent conformation when organized at the interface.

Please cite this article as: D.A. Peñalva, et al., Atypical surface behavior of ceramides with nonhydroxy and 2-hydroxy very long-chain (C28–C32) PUFAs, Biochim. Biophys. Acta (2013), http://dx.doi.org/10.1016/j.bbamem.2013.11.018

Table 2
Estimation of the organization of VLCPUFA-containing ceramides in monolayers.

Molecular species	Molecular dimension		LC phase (30 mN/m)		
	Acyl chains volume (V)[a] ($Å^2$)	Acyl chain length (L)[b] (Å)	Semi-empirical thickness[c] (Th) (Å)	L/Th	$\mu_\perp$[d] (mD)
n−28:4Cer	1292	22.7	16.6 ± 0.8	1.4 ± 0.1	832 ± 40
n−30:5Cer	1346	23.2	13.2 ± 0.8	1.8 ± 0.1	777 ± 25
n−32:5Cer	1400	24.3	11.2 ± 0.2	2.2 ± 0.1	1255 ± 10
h−28:4Cer	1292	22.7	22.0 ± 2.0	1.0 ± 0.1	360 ± 20
h−30:5Cer	1346	23.2	22.4 ± 0.4	1.0 ± 0.1	400 ± 18
h−32:5Cer	1400	24.3	14.4 ± 0.4	1.7 ± 0.1	668 ± 22
n−16:0Cer	969	18.4	23.6 ± 0.8	0.8 ± 0.1	551 ± 33
n−24:1Cer	1185	22.0	28.2 ± 0.2	0.8 ± 0.1	463 ± 25

[a] Calculated as the sum of the average volumes of the two asymmetrical hydrophobic Cer chains, obtained after Eq. (3).
[b] Calculated as the average of the two asymmetrical hydrophobic chain lengths, obtained after Eq. (4).
[c] Calculated as V/MMA.
[d] Calculated after Eq. (2).

3.5. Thermodynamic analysis of VLCPUFA-containing ceramides in monolayers

Lowering the temperature from 21 °C to 8 °C resulted, as expected, in a decrease of the π_t of VLCPUFA-containing Cer films since the latter condition favors the LC regime; this was complete in the case of the species with the longest fatty acids, n−32:5 Cer and h−32:5Cer (Table 3). The collapse pressure was less affected by this temperature difference. The integrated area under the π versus MMA curve gives information of the free energy of the compression process [10,13]. Since this parameter involves the entropy lost upon the increase of molecular packing order in the monolayer under compression, it is expected to be smaller at lower temperatures, as a more condensed state is favored than at higher temperatures. These effects, as well as an increase of the free energy of compression with the acyl chain length, are observed in Table 3. This supports the logical implication that the longer and more unsaturated the Cer acyl chains are, the larger the entropy lost upon compression is.

As a comparison, in early work [10] a free energy of compression of ~0.15–0.25 kcal mol^{-1} was reported for bovine brain Cer in the temperature range studied here. Our own calculations give values of 0.3 ± 0.1 kcal mol^{-1} for the more expanded 18:1 Cer and a very low value for the condensed 16:0 and 24:1 Cers (0.07 ± 0.01 kcal mol^{-1}). These values are far lower than those found here for the VLCPUFA Cer species, even for monolayers that are completely in the LC state (h−32:5 Cer and n−32:5 Cer at 8 °C). Most interesting was the comparison between the n-V and h-V Cer species, as the n-V Cer species showed larger free energy values than their h-V counterparts at the two temperatures studied. The larger free energies of compression observed for the n-V Cer species were consistent not only with their larger MMA, but also with their more diffuse phase transitions (see Fig. 2). This may reflect a lower capacity for close packing of the n-V Cer than of the h-V Cer species (Fig. 3 and Table 1). It is important to recall that the free energy of compression, besides entropic contributions, also contains a component related to the enthalpy change associated to the phase transformation. Thus, the difference may be a consequence of stronger interactions between the polar headgroups, in addition to a tighter acyl chain packing, of the h-V Cer than of the n-V Cer species.

One of the advantages of using the monolayer technique to study thermodynamic properties of lipids is that it requires small amounts of sample. The isolation in pure form of the Cer species containing n- and h-VLCPUFAfrom a natural source by the method described above is laborious and may result in very scarce amounts of the rarer species. This largely limits the possibility of performing thermodynamic analysis of these molecules organized as bilayer structures. However, their behavior in Langmuir monolayers may shed some light into their possible behavior if organized as bulk dispersions.

As previously proposed [10] the lower temperature at which a complete LE behavior is observed in monolayers (as obtained from the intercepts between the collapse pressure- and the π_t-temperature linear regressions) should be roughly in keeping with the melting temperature observed in bilayers (T_m). Thus, for a series of glycosphingolipids the agreement between the T_m experimentally determined by differential scanning calorimetry (DSC) and that estimated from monolayer measurements is remarkable [25]. On these bases, for 16:0 Cer suspended in bulk aqueous solution, a T_m of 93.2 °C was previously reported using DSC [5] and a T_m of 91.4 ± 1.4 °C can be estimated from extrapolation of monolayer transitions by the above-mentioned interception method [9]. This quite close agreement (within about 2 °C) led us to estimate an approximate T_m for the present VLCPUFA-containing Cer (Table 3). This method suggested T_m values of 45–46 °C for n- and h−28:4Cer, a higher value for the h−30:5Cer (53 °C) and a lower value for its n-V counterpart (36 °C).

As the n-V Cer is expected to undergo its phase transition at ~36 °C, it should presumably be organized as a low curvature interface, this estimation positions the T_m of the n−30:5Cer within the physiological temperature range and the rest of theVLCPUFA-containing Cer analyzed not far from such range. This suggests that in the cell membrane environment subtle changes of temperature, and/or a drop in π due to

Table 3
Thermodynamic parameters of VLCPUFA-containing ceramides in monolayer.

Molecular species	21 °C			8 °C			
	LE → LC transition pressure (π_t) (mN/m)	Collapse pressure (mN/m)	Compression free energy[a] (kcal/mol)	LE → LC transition pressure (π_t) (mN/m)	Collapse pressure (mN/m)	Compression free energy[a] (kcal/mol)	π_t-T vs. collapse π-T intersection (°C)
n−28:4 Cer	15 ± 2	39 ± 1	0.99 ± 0.05	6 ± 1	44 ± 1	0.72 ± 0.01	45 ± 4
n−30:5 Cer	23 ± 2	39 ± 2	1.64 ± 0.04	14 ± 1	45 ± 2	1.58 ± 0.05	36 ± 6
n−32:5 Cer	16 ± 1	47 ± 1	1.90 ± 0.03	–	45 ± 1	1.53 ± 0.01	–
h−28:4 Cer	15 ± 1	45 ± 2	0.72 ± 0.02	5 ± 1	48 ± 1	0.50 ± 0.01	46 ± 5
h−30:5 Cer	19 ± 1	42 ± 2	0.78 ± 0.04	11 ± 1	45 ± 1	0.53 ± 0.01	53 ± 3
h−32:5 Cer	5 ± 2	44 ± 1	1.00 ± 0.07	–	41 ± 1	0.66 ± 0.05	–

[a] Obtained by integrating the compression isotherms from 1 to 35 mN/m.

Please cite this article as: D.A. Peñalva, et al., Atypical surface behavior of ceramides with nonhydroxy and 2-hydroxy very long-chain (C28–C32) PUFAs, Biochim. Biophys. Acta (2013), http://dx.doi.org/10.1016/j.bbamem.2013.11.018

thermal fluctuation [33], could induce an LC → LE phase transition of these molecules, which, according to our results (Table 1), involves a large molecular lateral expansion. Since the Cer polar headgroup is very small (Fig. 1), such lateral expansion would concomitantly translate into changes of the overall geometry of the Cer molecules. As it was previously proposed [20,24], the geometrical properties of lipids are of paramount importance for the adoption of defined supramolecular structure. All Cers fall into the group of "inverted cone" shaped molecules; as a general rule, this characteristic should favor negatively curved structures, some of which promote membrane fusion events [17,25–27]. It remains to be evaluated if the long and bulk acyl chains of VLCPUFA-Cer may further enhance this effect compared to the more common species. Studies in this direction will provide evidences for a deeper understanding of the physiological importance of VLCPUFA-containing Cers during the acrosomal reaction, a process that requires the involvement of structural lipid intermediates with negative curvature.

Acknowledgments

This work was supported by FONCyT, CONICET, SECyT-Universidad Nacional de Córdoba, and SGCyT-Universidad Nacional del Sur (Argentina). FD, SSA, BM, MIA and MLF are career investigators and DAP is fellow of CONICET.

References

[1] M.I. Aveldano, M. VanRollins, L.A. Horrocks, Separation and quantitation of free fatty acids and fatty acid methyl esters by reverse phase high pressure liquid chromatography, J. Lipid Res. 24 (1983) 83–93.
[2] E.G. Bligh, W.J. Dyer, A rapid method of total lipid extraction and purification, Can. J. Biochem. Physiol. 37 (1959) 911–917.
[3] H.L. Brockman, C.M. Jones, C.J. Schwebke, J.M. Smaby, D.E. Jarvis, Application of microcomputer-controlled film balance system to collection and analysis of data from mixed monolayers, J. Colloid Interface Sci. 78 (1980) 502–512.
[4] H.L. Brockman, M.M. Momsen, R.E. Brown, L. He, J. Chun, H.S. Byun, R. Bittman, The 4,5-double bond of ceramide regulates its dipole potential, elastic properties, and packing behavior, Biophys. J. 87 (2004) 1722–1731.
[5] J.V. Busto, M.L. Fanani, T.L. De, J. Sot, B. Maggio, F.M. Goni, A. Alonso, Coexistence of immiscible mixtures of palmitoylsphingomyelin and palmitoylceramide in monolayers and bilayers, Biophys. J. 97 (2009) 2717–2726.
[6] F. Dupuy, M.L. Fanani, B. Maggio, Ceramide N-acyl chain length: a determinant of bidimensional transitions, condensed domain morphology, and interfacial thickness, Langmuir 27 (2011) 3783–3791.
[7] F. Dupuy, B. Maggio, The hydrophobic mismatch determines the miscibility of ceramides in lipid monolayers, Chem. Phys. Lipids 165 (2012) 615–629.
[8] M.L. Fanani, S. Hartel, B. Maggio, T.L. De, J. Jara, F. Olmos, R.G. Oliveira, The action of sphingomyelinase in lipid monolayers as revealed by microscopic image analysis, Biochim. Biophys. Acta 1798 (2010) 1309–1323.
[9] M.L. Fanani, B. Maggio, Phase state and surface topography of palmitoyl-ceramide monolayers, Chem. Phys. Lipids 163 (2010) 594–600.
[10] G.D. Fidelio, B. Maggio, F.A. Cumar, Molecular parameters and physical state of neutral glycosphingolipids and gangliosides in monolayers at different temperatures, Biochim. Biophys. Acta 854 (1986) 231–239.
[11] N.E. Furland, G.M. Oresti, S.S. Antollini, A. Venturino, E.N. Maldonado, M.I. Aveldano, Very long-chain polyunsaturated fatty acids are the major acyl groups of sphingomyelins and ceramides in the head of mammalian spermatozoa, J. Biol. Chem. 282 (2007) 18151–18161.
[12] N.E. Furland, S.R. Zanetti, G.M. Oresti, E.N. Maldonado, M.I. Aveldano, Ceramides and sphingomyelins with high proportions of very long-chain polyunsaturated fatty acids in mammalian germ cells, J. Biol. Chem. 282 (2007) 18141–18150.
[13] G.L. Gaines, Insoluble Monolayers at Liquid–Gas Interfaces, Interscience Publishers, New York, 1966.
[14] H. Hama, Fatty acid 2-hydroxylation in mammalian sphingolipid biology, Biochim. Biophys. Acta 1801 (2010) 405–414.
[15] Y.A. Hannun, L.M. Obeid, Many ceramides, J. Biol. Chem. 286 (2011) 27855–27862.
[16] S. Hartel, M.L. Fanani, B. Maggio, Shape transitions and lattice structuring of ceramide-enriched domains generated by sphingomyelinase in lipid monolayers, Biophys. J. 88 (2005) 287–304.
[17] J.M. Holopainen, M.I. Angelova, P.K. Kinnunen, Vectorial budding of vesicles by asymmetrical enzymatic formation of ceramide in giant liposomes, Biophys. J. 78 (2000) 830–838.
[18] J.M. Holopainen, H.L. Brockman, R.E. Brown, P.K. Kinnunen, Interfacial interactions of ceramide with dimyristoylphosphatidylcholine: impact of the N-acyl chain, Biophys. J. 80 (2001) 765–775.
[19] J.M. Holopainen, M. Subramanian, P.K. Kinnunen, Sphingomyelinase induces lipid microdomain formation in a fluid phosphatidylcholine/sphingomyelin membrane, Biochemistry 37 (1998) 17562–17570.
[20] J.N. Israelachvili, S. Marcelja, R.G. Horn, Physical principles of membrane organization, Q. Rev. Biophys. 13 (1980) 121–200.
[21] C. Lheveder, J. Meunier, S. Henon, Brewster angle microscopy, in: A. Baszkin, W. Norde (Eds.), Physical Chemistry of Biological Interfaces, Marcel Dekker, Inc., NY, 2000.
[22] X.M. Li, J.M. Smaby, M.M. Momsen, H.L. Brockman, R.E. Brown, Sphingomyelin interfacial behavior: the impact of changing acyl chain composition, Biophys. J. 78 (2000) 1921–1931.
[23] H. Lofgren, I. Pascher, Molecular arrangements of sphingolipids. The monolayer behaviour of ceramides, Chem. Phys. Lipids 20 (1977) 273–284.
[24] B. Maggio, Geometric and thermodynamic restrictions for the self-assembly of glycosphingolipid–phospholipid systems, Biochim. Biophys. Acta 815 (1985) 245–258.
[25] B. Maggio, The surface behavior of glycosphingolipids in biomembranes: a new frontier of molecular ecology, Prog. Biophys. Mol. Biol. 62 (1994) 55–117.
[26] B. Maggio, J. Albert, R.K. Yu, Thermodynamic-geometric correlations for the morphology of self-assembled structures of glycosphingolipids and their mixtures with dipalmitoylphosphatidylcholine, Biochim. Biophys. Acta 945 (1988) 145–160.
[27] B. Maggio, F.A. Cumar, R. Caputto, Induction of membrane fusion by polysialogangliosides, FEBS Lett. 90 (1978) 149–152.
[28] H.M. McConnell, Structures and transitions in lipid monolayers at the air–water interface, Annu. Rev. Phys. Chem. 42 (1991) 171–195.
[29] G.M. Oresti, P.L. Ayuza Aresti, G. Gigola, L.E. Reyes, M.I. Aveldano, Sequential depletion of rat testicular lipids with long-chain and very long-chain polyenoic fatty acids after X-ray-induced interruption of spermatogenesis, J. Lipid Res. 51 (2010) 2600–2610.
[30] G.M. Oresti, J.M. Luquez, N.E. Furland, M.I. Aveldano, Uneven distribution of ceramides, sphingomyelins and glycerophospholipids between heads and tails of rat spermatozoa, Lipids 46 (2011) 1081–1090.
[31] D.A. Peñalva, N.E. Furland, G.H. Lopez, M.I. Aveldaño, S.S. Antollini, Unique thermal behavior of sphingomyelin species with nonhydroxy and 2-hydroxy very-long-chain (C28–C32) polyunsaturated fatty acids, J. Lipid Res. (2013). Q2
[32] M.A. Perillo, A. Guidotti, E. Costa, R.K. Yu, B. Maggio, Modulation of phospholipases A2 and C activities against dilauroylphosphorylcholine in mixed monolayers with semisynthetic derivatives of ganglioside and sphingosine, Mol. Membr. Biol. 11 (1994) 119–126.
[33] M.C. Phillips, The physical state of phospholipid and cholesterol in monolayers, bilayers, and membranes, in: J.F. Danielli, M.D. Rosenberg, D.A. Cadenhead (Eds.), Progress in Surface and Membrane science, Academic Press, New York, 1972, pp. 139–221.
[34] S.N. Pinto, L.C. Silva, A.H. Futerman, M. Prieto, Effect of ceramide structure on membrane biophysical properties: the role of acyl chain length and unsaturation, Biochim. Biophys. Acta 1808 (2011) 2753–2760.
[35] A. Poulos, D.W. Johnson, K. Beckman, I.G. White, C. Easton, Occurrence of unusual molecular species of sphingomyelin containing 28–34-carbon polyenoic fatty acids in ram spermatozoa, Biochem. J. 248 (1987) 961–964.
[36] M. Rabionet, A.C. van der Spoel, C.C. Chuang, B. von Tumpling-Radosta, M. Litjens, D. Bouwmeester, C.C. Hellbusch, C. Korner, H. WIEGANDT, K. Gorgas, F.M. Platt, H.J. Grone, R. Sandhoff, Male germ cells require polyenoic sphingolipids with complex glycosylation for completion of meiosis: a link to ceramide synthase-3, J. Biol. Chem. 283 (2008) 13357–13369.
[37] B.S. Robinson, D.W. Johnson, A. Poulos, Novel molecular species of sphingomyelin containing 2-hydroxylated polyenoic very-long-chain fatty acids in mammalian testes and spermatozoa, J. Biol. Chem. 267 (1992) 1746–1751.
[38] M.B. Ruiz-Arguello, M.P. Veiga, J.L. Arrondo, F.M. Goni, A. Alonso, Sphingomyelinase cleavage of sphingomyelin in pure and mixed lipid membranes. Influence of the physical state of the sphingolipid, Chem. Phys. Lipids 114 (2002) 11–20.
[39] R. Sandhoff, Very long chain sphingolipids: tissue expression, function and synthesis, FEBS Lett. 584 (2010) 1907–1913.
[40] R. Sandhoff, R. Geyer, R. Jennemann, C. Paret, E. Kiss, T. Yamashita, K. Gorgas, T.P. Sijmonsma, M. Iwamori, C. Finaz, R.L. Proia, H. Wiegandt, H.J. Grone, Novel class of glycosphingolipids involved in male fertility, J. Biol. Chem. 280 (2005) 27310–27318.
[41] J.M. Smaby, V.S. Kulkarni, M. Momsen, R.E. Brown, The interfacial elastic packing interactions of galactosylceramides, sphingomyelins, and phosphatidylcholines, Biophys. J. 70 (1996) 868–877.
[42] J.M. Smaby, M.M. Momsen, H.L. Brockman, R.E. Brown, Phosphatidylcholine acyl unsaturation modulates the decrease in interfacial elasticity induced by cholesterol, Biophys. J. 73 (1997) 1492–1505.
[43] S.R. Zanetti, M.M. de Los Angeles, D.E. Rensetti, M.W. Fornes, M.I. Aveldano, Ceramides with 2-hydroxylated, very long-chain polyenoic fatty acids in rodents: From testis to fertilization-competent spermatozoa, Biochimie 92 (2010) 1778–1786.
[44] S.R. Zanetti, M.L. Monclus, D.E. Rensetti, M.W. Fornes, M.I. Aveldano, Differential involvement of rat sperm choline glycerophospholipids and sphingomyelin in capacitation and the acrosomal reaction, Biochimie 92 (2010) 1886–1894.

Please cite this article as: D.A. Peñalva, et al., Atypical surface behavior of ceramides with nonhydroxy and 2-hydroxy very long-chain (C28–C32) PUFAs, Biochim. Biophys. Acta (2013), http://dx.doi.org/10.1016/j.bbamem.2013.11.018